Computational method for general multicenter electronic structure calculations

P. F. Batcho*
Department of Chemistry and Courant Institute of Mathematical Sciences, New York University, Room 1021, 31 Washington Place, New York, New York 10003
and Howard Hughes Medical Research Institute, New York, New York 10003
(Received 16 November 1999)

Here a three-dimensional fully numerical (i.e., chemical basis-set free) method [P. F. Batcho, Phys. Rev. A **57**, 6 (1998)], is formulated and applied to the calculation of the electronic structure of general multicenter Hamiltonian systems. The numerical method is presented and applied to the solution of Schrödinger-type operators, where a given number of nuclei point singularities is present in the potential field. The numerical method combines the rapid ''exponential'' convergence rates of modern spectral methods with the multiresolution flexibility of finite element methods, and can be viewed as an extension of the spectral element method. The approximation of cusps in the wave function and the formulation of multicenter nuclei singularities are efficiently dealt with by the combination of a coordinate transformation and a piecewise variational spectral approximation. The complete system can be efficiently inverted by established iterative methods for elliptical partial differential equations; an application of the method is presented for atomic, diatomic, and triatomic systems, and comparisons are made to the literature when possible. In particular, local density approximations are studied within the context of Kohn-Sham density functional theory, and are presented for selected subsets of atomic and diatomic molecules as well as the ozone molecule.

PACS number(s): 02.70.−c, 31.10.+z

I. INTRODUCTION

The study of quantum mechanical properties of materials is central to a broad array of problems in chemistry and materials science ranging from molecular mechanics force field development to detailed electronic structure properties of molecules with several hundred nuclei and electrons. Material design challenges can benefit from reliable, robust, and accurate molecular simulations in fields ranging from the analysis of new pharmaceuticals and herbicides to biological systems such as amino acids, peptides, and complex crystalline structures for solid-state chemical application. As regards modeling, the theoretical chemical statement is addressed in two distinct steps; first a theoretical approximation to the Schrödinger or Dirac equation, and then a computational approximation for the numerical solution. The primary computational approach for *ab initio* quantum chemical methods has been the linear combination of molecular orbitals (LCAO), along with the dominant use of Gaussian chemical basis sets [1], and for solid-state calculations focus has been given to plane waves and pseudopotentials [2]. The nature of quantum mechanical operators and their solutions offer significant challenges ranging from large-scale system modeling requirements to rapidly varying wave functions in physical space and large gradients at nuclei locations. Numerical approaches must overcome such obstacles, and efficient methods must deal with wave function cusps at the nuclei locations as well as multicenter operator singularities. In the context of theoretical approximations, advanced treatments of electronic correlation, such as the coupled cluster method, have severe computational scalings to large systems, and a 100-fold improvement in computational capability is expected to yield only a factor of two improvement in the tractable system size [3]. Density functional theory provides an alternative to the approximate, in principle exact, treatment of electron exchange and correlation, and reduces the scaling problem; however, new computational approaches that capitalize on molecular scaling advantages are critical for the success of future electronic structure calculation. Here we apply a fully numerical high-precision computational method to general multicenter electronic structure calculations within the context of density functional theory [4].

Computational approaches that utilize locally centered global chemical basis sets, such as Gaussian functions, have demonstrated impressive chemical modeling capabilities for electronic structure calculations. In addition, systematic constructions of such basis sets for general molecular structures have achieved considerable success over the last few decades. However computational scalings to larger systems, and the difficulty of overcoming numerical truncation errors of finite expansions, are inevitable. Chemical accuracy is generally considered to be achieved at 10^{-3} hartree, since bonding interactions typically involve energy changes on the order of 10^{-1} hartree; for more discussion on favorable aspects of fully numerical approaches and the need for low numerical errors, see Refs. [6–8]. A disadvantage of finite global basis sets is the fact of low numerical errors, and this is a result of the slow (algebraic) and nonuniform convergence of the numerical approximation to the theoretical statement. For example, a systematic approximation of *s*-type hydrogenlike orbitals with an expansion of orthogonal Hermite polynomials, with their Gaussian weight function, yields errors of order $n^{-5/2}$ and errors of $n^{-3/2}$ in expectation values of the kinetic energy operator; here n is the size of the basis set expansion [5]. The fundamental success of finite chemical basis-set approximations lies in the ability to model, or approximate, the wave function's features with

*Electronic address: paul@biomath.nyu.edu

systematic expansions. Linear combinations of Gaussians with floating exponents, designed to optimize the expectation value of the Hamiltonian, have been shown to have subgeometric convergence; however, calculation of a new system requires a reoptimization of the exponents. High-precision diatomic calculations have recently been demonstrated with even-tempered basis sets [9], and required greater than 600 primitive basis elements for a N_2 $X\alpha$ calculation to achieve 10^{-6}-hartree errors in the total energy. The same basis set was then applied to similar diatomics to achieve a 10^{-3}-hartree errors in total energies; calculations with such basis sets beyond the diatomic level are not known to the author.

For LCAO calculations, care in systematically clustering basis-set information near the nuclei must be exercised to achieve chemical accuracy [5]; in addition, algebraic convergence rates in finite basis-set expansion errors can be expected in locally centered global expansions. In the case of solid-state calculations a resolution fine enough to properly approximate core wave functions requires millions of plane waves for the simplest silicon unit cell. The nonuniform convergence of global basis-set errors will generally focus Gibbs-type oscillations near the nuclei cusp regions, and the algebraic convergence can cause misleading results with finite-dimensional sets [10,11]. Given the algebraic convergence rates of Gaussian basis sets, particularly when contraction sets are used, a question can be posed as to the numerical error estimates involved with such methods. Does an extremely small chemical modeling improvement from a 6-311++$G(d,p)$ basis to a 6-311++6(2*df*,2*p*) set represent a well converged solution, or is it an artifact of the rate of convergence for the approximation, irrespective of correlation treatment? Numerical challenges continue to remain for heavy nuclei and transition metal calculations, as well for the direct material property prediction. It is desirable to have a systematic high-precision computational approach that can deal with the multiresolution and high-precision numerical needs of quantum mechanical wave functions. A physical space domain decomposition is used here, and systematic generations of computational meshes are discussed for the optimal approximation of the wave function and assessment of numerical accuracy.

Here a fully numerical (chemical basis-set free) domain decomposition method, the molecular spectral element (MSE) method [4], is presented and applied to polyatomic systems. With the MSE method no assumptions beyond the stated Hamiltonian are used and the LCAO method, plane-wave basis, pseudopotentials, Gaussian basis, and Slater-type orbitals have all been avoided. The MSE has its roots in the spectral element method described in Refs. [12–14]. The MSE computational method combines rapid ''exponential'' convergence rates of modern spectral methods with the multiresolution flexibility of finite element methods, and can be viewed as an extension of the spectral element method. A variational formulation is applied to the operator, and the nuclei singularities are efficiently captured by a local coordinate transformation. The variational formulation preserves the symmetry of the operator, and allows an efficient inversion. In addition, the formulation of the variational statement and the coordinate transformation for the singularity produces a method that can effectively deal with operator singularities as high as r^{-p}, $p<3$, in three dimensions.

The computational approach discussed in this paper can be applied to the various quantum chemical theoretical approximations, including Hartree, (post)Hartree-Fock, Hartree-Fock-Slater, and density functional theory (DFT) methods; however, focus is given to the density functional formulation. Within the context of the density functional formulations Hohenberg-Kohn-Sham (KS) theory [15,16], established a firm theoretical foundation for minimizing an energy functional over a space of single-particle orbitals for electronic structure systems. In recent years the quantum chemistry community has found a notable improvement from the results of DFT over those found from Hartree-Fock results, particularly if nonlocal approximations are used. They are comparable, if not better results, as compared to Gaussian-MP2 methods [17–20]. The fact that KS-DFT is formulated as a single-particle Schrödinger equation makes it particularly attractive within the context of modern numerical methods for solving elliptic partial differential equations. Here we present a state-of-the-art numerical method for solving the general single-particle Schrödinger equation, and offer the unambiguous assessment of the various theoretical approximations within the quantum chemical theoretical statement. The single particle exchange-correlation potential $V_{\mathrm{xc}}(\mathbf{x})$, is defined by a suitable DFT model that is only a function of the electron density function $\rho(\mathbf{x})$ in local approximations. In nonlocal approximations the potential can have a strongly nonlinear dependence on the electron density and its gradient, $V_{\mathrm{xc}}(\mathbf{x},\rho(\mathbf{x}),|\nabla\rho(\mathbf{x})|,\ \nabla^2\rho(\mathbf{x}),\ldots)$. The Kohn-Sham equations are given in Eqs. (1)–(4), stated in atomic units (a.u.), for general gradient approximations in spin compensated form:

$$-\tfrac{1}{2}\nabla^2\varphi_p(\mathbf{x})+[J(\mathbf{x})-V(\mathbf{x})]\varphi_p(\mathbf{x}) + V_{\mathrm{xc}}(\rho(\mathbf{x}),|\nabla\rho(\mathbf{x})|,\nabla^2\rho(\mathbf{x}))\varphi_p(\mathbf{x})=\varepsilon_p\varphi_p(\mathbf{x}) \quad \text{in } \Omega^3 \tag{1}$$

$$(\varphi_i,\varphi_j)=\int_\Omega \varphi_i(\mathbf{x})\varphi_j(\mathbf{x})d\mathbf{x}=\delta_{ij}, \tag{2}$$

where

$$V(\mathbf{x})=\sum_{p,j}\frac{Z_j}{\mathbf{r}_{pj}}, \tag{3}$$

$$J(\mathbf{x})=\int_\Omega\frac{\rho(r')}{|r-r'|}dr', \quad \rho(\mathbf{x})=2\sum_a|\varphi_a(\mathbf{x})|^2, \tag{4}$$

where $r_{ij}^2=(x_i-x_j)^2+(y_i-y_j)^2+(z_i-z_j)^2$, Z_j are the atomic numbers of the individual nuclei, and ε_p and $\phi_p(\mathbf{x})$ are the molecular orbital energy and its wave function in physical space. The MSE method eliminates the use of global basis sets, and approaches the solution of the quantum mechanical equations from a variational domain decomposition approach where high-order polynomial approximations are made within each subdomain. In addition to the rapid decay of the numerical error the collocation character of the MSE method computes the molecular orbitals directly in

physical space rather than the coefficients of a series expansion for a given orbital. Advantages are therefore found in the solution's rapid evaluation and in the elimination of inverse mappings for LCAO basis-set expansions that can be several million in size. In general, grid based methods offer many times more functions to minimize with respect to the Hamiltonian. These functions are highly localized in space, and thus advantages can be found with the multiresolution aspects of the wave function. Similarly the structure of the resulting linear algebra statement offers computational tractability with regards to operator evaluations for large systems.

The MSE method can be viewed as a spectral element method that is adapted to treat the operator r^{-1} singularities and cusps in the solutions that arise at the nuclei locations. Attempts in the past to use finite element methods [21–24] have either dealt only with diatomic molecules where the singularity can be removed through using spherical or prolate-spheriodal coordinates, or alternatively a use of the integral transform of r^{-1} was employed. A three-dimensional finite element approach was applied to H_3^{++} [25], for algebraic converging formulations; the correct treatment of the singularity was bypassed, since a low-order formulation tends to keep the remaining solution somewhat isolated from the errors near the core. Of special interest is the work on applying *p*-type finite elements to H_3^{+} electronic structure calculation [26,27]; this work will be discussed in more detail in Sec. II A. However, the advantages of going to local methods versus global expansions have been recognized in these previous studies. These include advantages in computational scalings to large molecules, improved accuracy of spatial moments, $\langle \mathbf{r}^p \rangle$, and gradients which are strongly dependent on wave function accuracy. In general the error in the total energy is an insensitive criterion for judging wave function accuracy [23], which is critical for reliable prediction of material properties.

Of particular interest in the context of finite element formulations is the linear scalability of the computational approach with respect to molecular complexity. For the solution of the molecular orbitals global chemical basis-set expansions exhibit either cubic or quartic scaling with respect to the dimension of these basis sets. The physical space formulation of the MSE method combined with the domain decomposition character offers the complete elimination of multicenter complexity for operator evaluations, e.g., a systematic application of the MSE method has a uniform numerical approximation over a wide range of molecular structures, and the computational work scales linear with the number of subdomains, which scales linear with the number of nuclei. Within the context of density functional theory the LCAO method scales with the third power of the number of nuclei. Recently, efforts at an *asymptotic* linear scaling of DFT formulations have been studied within the context of density matrix truncation approximations in physical space [28–31]. A systematic application and study of these methods can in principle be combined with the efficient domain decomposition method addressed in this paper; however, the MSE is naturally linear with respect to the number of nuclei for the computation of the expectation values of the full Hamiltonian. With the MSE domain decomposition method, future algorithm developments with multilevel and Krylov space methods can lead to linear scaling in electrons as well, and therefore a total linear scalability is realizable for high level quantum mechanical simulation. The multiresolution flexibility of the domain decomposition method is also noteworthy in cases where heavy nuclei have large localized gradients near the nuclei location, in combination with the valence orbitals which tend to have more diffuse solutions throughout the molecule. The method presented here has the geometric flexibility to deal with both types of solutions within a given optimal domain decomposition, and, in some sense, is natural to the formulation. Noteworthy are recently introduced wavelet approximations which are designed to capitalize on the multiresolution aspects of the wavelet basis [32], as well as recent finite difference formulations within the context of a pseudopotential formulation [33]. The MSE formulation offers a consistent and rapidly convergent approximation of the full Hamiltonian, which accurately captures the balance of the kinetic energy and divergent terms in the near nuclei region. A more detailed discussion on the MSE numerical formulation can be found in Ref. [4], where various approaches were examined and exponential convergence rates were demonstrated for suitable benchmark cases.

In the context of the LCAO method a pseudospectral method has been applied to electronic structure calculations [34]. The use of collocation has shown to have advantages with regards to the computational complexity of the multicentered integrals via sum factorization techniques. However, the pseudospectral method still suffers from the drawbacks of the algebraic convergence of the expansion and the optimal choice for chemical basis sets. Here we adopt a somewhat universal basis set in a local region of physical space, and rapid convergence is guaranteed in terms of the size of the expansion. A method that extends fully numerical approaches to a multicenter system was formulated in Ref. [35], where each nucleus is treated as a separate solution with its own spherical coordinate system, and the individual solutions are added together by a defined weighting function. The individual treatment of nuclei in general mirrors global basis-set multicenter complexity, and the introduction of an additional nuclei requires the addition of a full atomic grid. Here we avoid these issues with a unified grid under the the context of a domain decomposition method which incorporates a systematic implementation of rapidly converging polynomial basis-set approximations. With the MSE approach the addition of a nuclei requires less then one tenth of an atomic grid, and highly efficient iterative methods with enhanced parallel processing advantages can be systematically employed for the wave function solution. Here a significant departure is made from the above methods in mathematical formulation and iterative methods used for solving the various eigensystems. The domain decomposition coupled with tensor (or warped) product forms of Lagrangian interpolants and Gaussian quadratures make the present formulation superior to classical finite element and finite difference based methods. The computational method used offers significant advantages where the total energy can be minimized via established Krylov space and multilevel methods, where no direct operator inversions are required. The MSE method offers an efficient treatment of the nuclei singularities with a seamless numerical matching to the remaining physical domain; and numerical errors are a direct con-

sequence of the degree of the polynomial used in the approximation as well as the physical size of the local domains.

In Sec. II we briefly review the spectral element method, and an adaptation to deal with the nuclei singularities. Discussions on the coordinate transformation of the singularity and the resulting algebraic system are presented. Section II C discusses various iterative methods for the solution of the molecular orbitals with the MSE approach, as well as expected scalings with molecular complexity. In Sec. III, results of atomic, diatomic, and triatomic systems are presented. The hydrogenlike solution of atomic nitrogen and zinc are presented in Sec. III A; exponential convergence is demonstrated with respect to the $1s$ and $2s$ orbitals. Section III B presents a local density approximation (LDA) $X\alpha$ calculation of diatomic nitrogen, and comparisons are made to highly accurate solutions presented in the literature for a finite element solution using prolate-spheriodal coordinates. In addition, the calculation of O, Ar, N_2, O_2, and F_2 are presented for the Vosko-Wilk-Nusair (VWN) LDA approximation. In Sec. III C, a study of the ozone molecule is made for the cyclic and ground state geometries under the $X\alpha$, Gunnarsson-Lundqvist (GL) empirical correlation correction, and VWN LDA approximations. Detailed total energies and molecular orbital structures and energies are presented, and comparisons are made to the various calculations discussed in the literature. In particular, we find that all closed shell LDA models predict the ground state to have a lower total energy, and that the $X\alpha$-VWN model in its paramagnetic closed shell limit predicts the experimental ionization potential to within a 2% error. In Sec. IV, we conclude with discussions on the overall numerical approach when used for quantum chemical calculations, and suggest several possibilities for future algorithm development and application to electronic structure calculations.

II. FORMULATION

A. Molecular spectral element method

The spectral element method is designed to solve elliptic boundary value problems in general complex domains by partitioning the given domain into quadrilaterials; spectral elements. Within each element the solution is approximated by Lagrangian interpolant polynomials, where tensor product forms are used. The first step in the procedure is to employ a variational formulation of the problem,

$$\frac{1}{2}\int_{\Omega_k}\nabla U(\mathbf{x})\cdot\nabla\phi(\mathbf{x})d\mathbf{x}+\int_{\Omega_k}\hat{V}(\mathbf{x})U(\mathbf{x})\phi(\mathbf{x})d\mathbf{x} = -\varepsilon\int_{\Omega_k}U(\mathbf{x})\phi(\mathbf{x})d\mathbf{x}, \tag{5}$$

where $U(\mathbf{x})$ is the chosen test function, and $\hat{V}(\mathbf{x})$ is the total single particle potential, $\hat{V}(\mathbf{x})=V(r)+2J(r)-V_{\mathrm{xc}}(\mathbf{r})$. Next interpolation points are chosen to define the basis set via the Lagrangian interpolants; in the standard spectral element formulation Gauss-Lobatto Legendre (GLL) points are chosen. The solution is expanded in terms of the higher-order polynomial interpolants $h_i(\xi)$,

$$\phi(\eta,\xi,\zeta)=\phi_{ijk}h_i(\eta)h_j(\xi)h_k(\zeta), \tag{6}$$

where (η,ξ,ζ) are the coordinates in the cubic space defined from an isoparameteric mapping. The test functions are also chosen as the interpolants, as in the traditional Galerkin formulation. In the case of deformed geometries the boundary is also expanded in GLL interpolants, and the GLL numerical quadrature is chosen to coincide with the interpolation points; therefore the interpolants are defined by $h_i(\xi_J)=\delta_{ij}$; this gives the method a collocation-type character. This choice of quadrature points and basis sets forms a discrete system of algebraic equations with a large degree of sparseness, and the use of tensor product forms result in efficient sum factorization techniques for operator evaluations [12–14]. The exponential convergence property, associated with polynomials from the singular Sturm-Liouville operators, gives the method a significant advantage over traditional finite element and finite difference methods. In large-scale applications several orders of magnitude less grid points are needed for the same accuracy when compared to traditional low-order methods; if needed, highly accurate solutions can be obtained at relatively little cost. The spectral element method has been used in three-dimensional time dependent solutions of fluid flow as well as large-scale solutions of eigensystems of coupled partial differential equations [36–39].

There are a number of obstacles that must be overcome in order to apply such a method to Schrödinger-type operators and electronic structure calculation. The molecular spectral element is formulated to deal with the numerical difficulties of a finite number of arbitrary spaced cusps and point singularities. The combination of geometric flexibility and exponential convergence rates yields a well-suited technique for solving Schrödinger-type operators. The singularity was found to be effectively handled by a coordinate transformation [4]. Where the integration of nuclei singularities can be subdivided into the integration over six square based pyramids. The transformation $\hat{x}=x$, $y=xu$, and $z=xw$ reduces the integration over a pyramid,

$$\int_0^1 dx\int_{-x}^{x}dy\int_{-x}^{x}dz r^{-1}\phi(x,y,z)\quad\text{in }\Omega^3, \tag{7}$$

to the evaluation of integrals of the form

$$\int_0^1 dx\int_{-1}^{1}du\int_{-1}^{1}dw\frac{x\phi(x,xu,xw)}{\sqrt{1+u^2+w^2}}\quad\text{in }\Omega^3. \tag{8}$$

Thus we partition the volume around the singularity with a cube and subdivide the cube into six pyramids; see Fig. 1. The transformation removes the singularity and smooth integrands remain which can be efficiently integrated with produce Gauss-Jacobi quadratures. This type of domain decomposition is somewhat optimal for solutions that are approximately spherically symmetric around the singularity, and tends to substantially reduce the number of elements needed to fill the remaining domain.

The last aspect in the formulation is an efficient approximation scheme for the transformed function $\phi(x,xu,xw)$ and the matching to adjacent quadrilaterials. The use of a Gauss-type quadrature over the cubic domain in the mapped

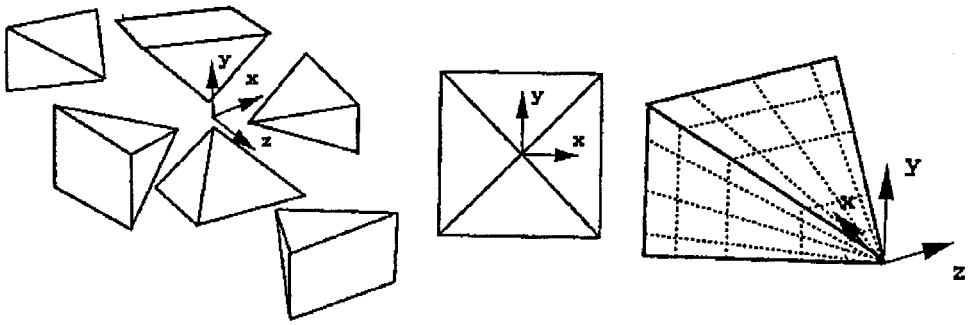

FIG. 1. An illustration of the pyramid decomposition of a cubic region around the singularity. The solution within the pyramids is represented by tensor product forms of appropriately chosen Gauss-Jacobi Lagrangian interpolants, and is routinely patched to adjacent quadrilaterial spectral elements.

space $(\hat{x},u,w)$ leads to integration points which can be used to form Lagrangian interpolants in a similar fashion as is done in a traditional spectral element scheme. The optimal approximation scheme was found to be the tensor product form of Lagrangian interpolants in the mapped space $\phi(x,xu,xw)=\phi_{ijk}h_i(\hat{x})h_j(u)h_k(w)$. A choice of GLL quadrature is used for the u and w components. This formulation allows a straightforward C^0 matching of the pyramid based system to the adjacent quadrilaterial of the spectral element method. For an optimal x-component numerical quadrature, the x weight was included in the choice of an integration rule, which did not include the vertex as an integration point [40]; similar types of quadrature rules were described in Ref. [41]. The discrete Laplacian mapping is formulated by using the mapped physical space gradients in the space $(\hat{x},u,w)$. With application of the chain rule we arrive at[1]

$$\frac{\partial}{\partial x}=\frac{\partial}{\partial\hat{x}}-\frac{u}{x}\frac{\partial}{\partial u}-\frac{w}{x}\frac{\partial}{\partial w}, \tag{9}$$

$$\frac{\partial}{\partial y}=\frac{1}{x}\frac{\partial}{\partial u}, \tag{10}$$

$$\frac{\partial}{\partial z}=\frac{1}{x}\frac{\partial}{\partial w}. \tag{11}$$

The gradients in the mapped space $(\partial/\partial\hat{x},\partial/\partial u,\partial/\partial w)$ are formulated within the context of a Gauss-Jacobi-Lagrangian interpolant derivative matrix in the $(\hat{x},u,w)$ space, as in the spectral element formulation. Here the x component of the discrete Laplacian is given:

$$A^x_{lmnijk}\phi_{ijk}=\int\int\int\frac{\partial}{\partial x}[h_l(\hat{x})h_m(u)h_n(w)]\frac{\partial}{\partial x}[h_i(\hat{x})h_j \times(u)h_k(w)]\phi_{ijk}x^2 d\hat{x}\,du\,dw \quad \text{in} \quad \Omega^3 \tag{12}$$

This leads to a variational formulation of the Laplacian with condition numbers in agreement with the convergence estimates of traditional spectral element methods for the variable coefficient Helmholtz equation [42]. The algebraic system is given in Eqs. (13) and (14) for the discrete system for Eqs. (1) and (2) respectively:

$$[\tfrac{1}{2}\mathbf{A}+\mathbf{B}_v]\phi_i=-\varepsilon_i\mathbf{B}\phi_i, \tag{13}$$

$$\phi_i\mathbf{B}\phi_j=\delta_{ij}, \tag{14}$$

where $\mathbf{A}$ is the sparse discrete Laplacian, $\mathbf{B}_v$ is a diagonal mass matrix weighted by the total single particle potential, $\mathbf{B}$ is the diagonal mass matrix, and ϕ_i is the algebraic vector of physical space mesh values of the ith computed orbital. The total matrix is never actually constructed in the iterative inversion methods suggested here, and parallel algorithms based on element partitioning can be efficiently implemented. The single particle potential is routinely evaluated on the spectral element mesh points, and evaluations of spatial derivatives pose no obstacles for implementing generalized gradient based DFT formulations. The complete system was efficiently inverted by the preconditioned conjugate gradient method, and exponential convergence rates in numerical approximations were demonstrated for suitable benchmark problems in cubic domains [4].

For a multicenter application the domain is decomposed into six pyramids around each nuclei, with quadrilaterials in the remaining domain. Within each pyramid the solution is decomposed into a tensor product form of Gauss-Jacobi Lagrangian interpolants. Typical meshes may consist of a box divided into quadrilaterials with elliptical shells placed around them, which are also divided into quadrilaterials (see Figs. 3 and 7); such meshes are routinely generated for molecular application. With the MSE method the dependence of the computational complexity on the number of nuclei is only felt through the number of elements needed to partition the domain. For example, in some circumstances a molecular system with five nuclei may have the same, or nearly the same, number of elements as a ten nuclei system; in this case the computational work is the same, given the same number of occupied orbitals. The operation count of the product of the DFT Hamiltonian with a given molecular orbital scales $\sim KN^4$, where K is the number of subdomains and N is the number of quadrature (collocation) points in one spatial direction, in a single subdomain. This operation is the primary computational expense of a given iteration were $N\sim 5-10$ and $K\sim 100-1000$ for moderate sized molecules.

Finally we comment on the work on applying p-type finite elements to electronic structure calculations for H_3^+ [26,27]. The work in Ref. [26] formulated a variant of the spectral element technique for use in Hartree-Fock calculations, and correctly isolated a key aspect of the formulation, namely, the tensor product forms and sum factorization technique for

[1]Correctly stated here versus those described in Ref. [4].

operator evaluations. However, the use of GLL interpolants was *not* used with its associated GLL quadrature rule, and this resulted in the loss of the highly favorable collocation character of the formulation, which allows the solution to be computed directly in physical space. This mismatch leads to significantly increased computational work, as well as a degraded conditioning of the algebraic system with increasing N. The approach was then modified to deal with three-dimensional point singularities via a variant of the Duffy transformation [27], as independently used in Ref. [4]. However in Ref. [27] the singularity was formulated as to be surrounded by cubes rather then pyramids, and again the collocation formulation was not used. The cubic domain decomposition was actually an early formulation tried in Ref. [4], and was discarded due to poor conditioning of the algebraic system with increasing N, as well as a less optimal domain decomposition for electronic structure calculations. The mismatch in the interpolant and quadrature points leads to several unsatisfactory results in the computational method, and is avoided by the MSE approach. The ability to efficiently use high degree polynomials is a primary motivation for the spectral element method. Here we demonstrate that p-type finite elements are a viable numerical approach to multicenter many electron systems with highly nonlinear functionals and strongly nonspherically symmetric wave functions in the near nuclei region.

B. Global energy minimization

The use of iterative methods for high-order finite element formulations is an established area in computational mathematics and advances from various multidisciplinary fields are expected to offer a rapid optimization of the iterative solver through the direct exchange of computational algorithms. Given a consistent and rapidly convergent spatial discretization an efficient algorithm must be formulated to solve the nonlinear coupled system of partial differential-integral equations of interest. The spectral element method has been implemented in connection to the inverse Lanczos method for the calculation of the lowest eigenpairs of coupled partial differential equations [38,39]. In the context of electronic structure calculation there has been a considerable amount of literature on the subject of iterative solvers that somewhat bypass the direct inverse iteration method [43–45]. Krylov methods, based on preconditioned conjugate gradient (PCG) iteration, are growing in popularity [44], and multilevel methods have found application in electronic structure and scattering applications [46–48]. The use of a physical-space domain decomposition method separates the complexity scaling with respect to the number of nuclei and the number of electrons. It is clearly linear in the number of nuclei, which only effects the number of subdomains (spectral elements) used. The scaling in number electrons is a function of the iterative eigensolver, and at worse scales square with number of electrons. The square scaling comes from the use of the Krylov method and needed orthogonalization reenforcement; with a further algorithm developed, Krylov methods can (in principle) be made linear with the number of electrons; i.e., the DFT self-adjoint operator gives a tridiagonal Hermitian matrix, and a selective reorthogonalization can be employed. Multilevel methods have been applied within the context of spectral element methods [14], and recently on modeled quantum chemical systems of equations [46]. It has been shown that a linear scaling relation with respect to the number of electrons can be expected. Typically multilevel methods are more attractive for nonlinear systems, and offer high efficiency, particularly for low aspect ratio elemental domains.

Here the iterative solver has not been optimized or extensively studied, and is therefore not discussed in significant detail. However, a fairly straightforward PCG implementation worked robustly for the molecular structures studied. Future efforts are focused at optimal iterative solvers and improvement of several orders of magnitude in both initial conditions and iterative efficiency can be expected; we expect a linear scaling in the number of orbitals with the use of multilevel methods. The general procedure is to obtain a solution of $[\mathrm{H}-\varepsilon_i]\varphi_i=0$, where the operator and energies are updated at each global iteration, and previous iterations are used as an initial guess $[\mathrm{H}^n-\varepsilon_i^n]\delta\varphi_i^{n+1}=-[\mathrm{H}^n-\varepsilon_i^n]\varphi_i^n$. At present a few hundred global iterations are necessary to obtain accurate total energies, and the overall iteration procedure is similar to that of Ref. [43], where each global iteration was performed by a mode by mode minimization. Each global mode iteration utilizes a predetermined number of inner PCG iterations before the operator is modified; here the preconditioner was taken as the diagonal of the discrete Laplacian. This choice of preconditioner was found to lead to scalings in the condition number of the overall system, in agreement with the traditional spectral element method. The computational complexity of the Hamiltonian matrix vector multiply with the discrete orbital scales proportional to KN^4 for the pyramid as well as the quadrilaterial decompositions, where K is the number of elements in the domain. At present each global iteration includes a complete reorthogonalization of the eigensystem. With the use of explicit updates [Eq. (15)] of the electron density, there has been no indication of charge sloshing instabilities by this method:

$$\rho^{n+1}(\mathbf{x})=\sum_{j=0}^{J_e}\beta_j\rho^{n-j}(\mathbf{x}),\quad \sum_j\beta_j=1. \tag{15}$$

The number of inner iterations is typically 5–30, depending on the numerical resolution; a lower resolution implies a lower number of inner iterations for optimal convergence. There are several different approaches to the use of PCG, and the optimal approach will remain under investigation. In particular, interest is given to recent work on nonlinear conjugate gradient methods [49], advances in large-scale implicitly restarted Arnoldi methods [50], and the very promising use of multilevel methods [46]. In general, it has been found that the treatment of the nonlinear minimization as a quasi-steady eigenproblem can allow the iterative solution to lock into local solutions, particularly if the electronic wave function is nearly degenerative. Care must be taken in an evaluation of the Coulomb potential during the iterative minimization and is discussed in Sec. II C.

C. Evaluation of the integral operators

The above formulation gives a numerical method that can effectively deal with Schrödinger-type operators, and will give exponential convergence rates in the numerical approxi-

mation. The Coulomb and exchange potentials must also be evaluated with exponential rates of convergence, and must be computationally tractable for large systems. The use of the PCG method has proven to be an efficient iterative method for the solution of Poisson's equation; diagonal preconditioning is typically used. The Coulomb operator $J(r)$ is formulated as

$$J(r)=\int_{\Omega}\frac{\rho(r')}{|r-r'|}dr', \tag{16}$$

$$\nabla^2 J(\mathbf{x})=-4\pi\rho(\mathbf{x}) \quad \text{in } \Omega^3. \tag{17}$$

The integral operators are solved via Poisson's equation; the operation count for a typical Poisson solve is $\sim MKN^4$. The operation count for a direct integration of the Coulomb operator is naively K^2N^6. Here M is the number of PCG iterations, typically 100–300, and one can expect, for complex molecules, that $K\sim 10^3$; this gives the Poisson solution method roughly a 10^2 advantage. For the Hartree-Fock exchange operator this also holds; however, there are N_α^2 Poisson solves required for each operator evaluation, N_α being the number of occupied molecular orbitals. Thus a considerable amount of work can be saved by efficient preconditioning of the discrete Laplacian, as well as the Helmholtz operator, in iterative solvers for the spectral element formulation [51]. The use of iterative solutions of Poisson's equation offers the efficient use of the previous solution as an initial guess within the global iterative method, as well as adaptive control over iterative solution residual levels. Here the Coulomb operator is solved to an iterative residual level of roughly one order of magnitude below the largest operator residual level, $\max_{i\neq j}(\phi_i^n,\mathrm{H}^n\phi_j^n)$. This effectively caused the computation work for the update of the Coulomb operator to be less intensive than the update of a given orbital. The partial PCG iterative solution for the Coulomb potential is effectively the energy minimization discussed in Ref. [32].

Boundary conditions for the potentials are also a key issue. The application of homogeneous Dirichlet boundary conditions on a finite domain are not as well suited for the potentials, since linear decay is present versus exponential decay for the orbitals. The use of multipole expansions on the boundary has proven effective for application of far-field Dirichlet boundary conditions [23,52]. Here the electron density is expanded around the computed center of charge for the molecule, and expansions up to quadrupole moments are considered. For application to molecular systems the rapid decay of the electron density and the smooth variation in the farfield make the multipole expansion a well suited method for potential boundary conditions. Chemical accuracy was routinely achieved with a single centered quadrupole expansion; however, the potential boundary condition can be considered to be the limiting factor in accuracy for the exact (machine accurate) wave function solution. This formulation has been implemented with negligible cost to the inversion of the Laplacian, and is discussed in Sec. III. Future application of more refined Green's function methods [53] could offer higher precision; alternatively, higher-order multipole expansions would be employed. Recently efforts at formulating and applying a semi-infinite spectral element approach for the far-field solution have shown promise, and will eliminate the needed for the multipole approximation, as well as decrease the total number of spectral elements by roughly an order of magnitude. Periodic structures, of course, have no limitation on solution accuracy for the application of potential boundary conditions.

III. RESULTS

There has been a large body of research on evaluations of LDA models for small molecular systems [35], and predictive capabilities continue to improve. Here we choose a subset of the historically challenging systems, and focus on the advantages of the physical space domain decomposition method in both solution interpretation and robust numerical properties. The results of three-dimensional LDA correlation potentials and chosen benchmark solutions are presented for O, Ar, O_2, N_2, F_2, and O_3, as well as hydrogenlike orbitals of N and Zn. The LDA-KS potentials are defined from the $X\alpha$ method of Eq. (18), the GL empirical correlation correction given in Eq. (19), [54], and the VWN correlation model in Eq. (20) taken from Refs. [19], [55]. All LDA models are taken in their paramagnetic closed shell limits, and α is taken to be an adjustable constant:

$$V_x^{\mathrm{LDA}}(\mathbf{x})=-\frac{3}{2}\alpha\left[\frac{3}{\pi}\rho(\mathbf{x})\right]^{1/3}, \tag{18}$$

$$V_{xc}^{\text{LDA-GL}}(\mathbf{x})=V_x^{\mathrm{LDA}}\beta(r_s), \tag{19}$$

$$V_{xc}^{\text{LDA-VWN}}(\mathbf{x})=V_x^{\mathrm{LDA}}(\mathbf{x})+\varepsilon_c(r_s,0)-\frac{r_s^{1/2}}{6}\frac{\partial\varepsilon_c^p}{\partial x}, \quad x=r_s^{1/2}, \tag{20}$$

where $\beta(r_s)=1+0.054r_s\ln(1+11.4/r_s)$, $r_s=[3/4\pi\rho(\mathbf{x})]^{1/3}$, for the details of Eq. (20), see Refs. [19], [55]. The total energies reported for the MSE-LDA results were computed by solving the electronic problem for the orbital energies and adding the nuclear/nuclear contribution [Eq. (21)],

$$E_T=2\sum_i \varepsilon_i-\tfrac{1}{2}\int\int\frac{\rho(\mathbf{r})\rho(\mathbf{r}')d\mathbf{r}\,d\mathbf{r}'}{|\mathbf{r}-\mathbf{r}'|}-\int[\rho(\mathbf{r})V_{\mathrm{xc}}(\mathbf{r})]d\mathbf{r}+E_{\mathrm{xc}}(\rho(r))+\sum_A^{\text{nuclei}}\sum_{B<A}\frac{Z_AZ_B}{R_{AB}}, \tag{21}$$

where $E_{\mathrm{xc}}(\rho(\mathbf{r}))=\int\rho(\mathbf{r})\varepsilon_{\mathrm{xc}}(\rho(\mathbf{r}))dr$. In addition to the LDA approximation a post-Langreth-Mehl gradient correction (LMGC) is applied to the LDA KS orbital solution. The post KS correction is presented here to parallel current work in LDA spin formulations [35]. However, the MSE computational approach has no numerical limitations for the calculation of fully self-consistent solutions with gradient corrections applied to the exchange-correlation potential; these results will be reported in future publications. For accurate thermochemical predictions LDA spin formations are generally needed. The LMGC correction to the total energy is given in Eq. (22) where $a=0.004\,28$, $f=b(|\nabla\rho|/\rho^{7/6})$, and $b=0.26$:

$$E_{\mathrm{xc}}=a\int\frac{(\nabla\rho)^2}{\rho^{4/3}}\left(e^{-F}-\frac{7}{18}\right)d\mathbf{r}. \tag{22}$$

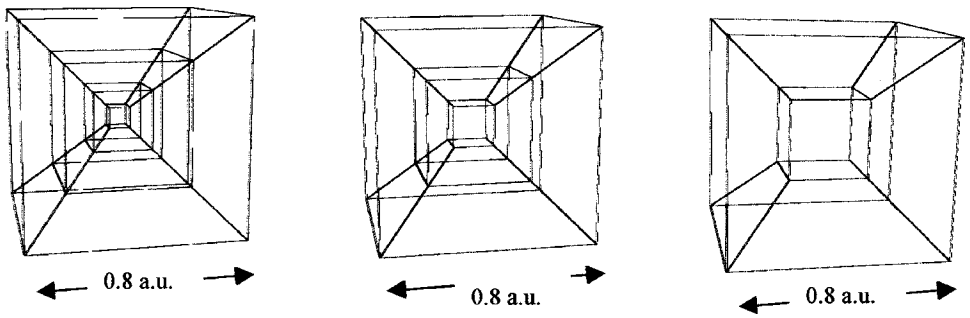

FIG. 2. The three near nuclei domain decompositions used for a calculation of the hydrogenlike orbital solutions for $Z=7$ and 30. This domain decomposition is typical of all calculations reported here. Typically a cube with an edge length of approximately 1.0 a.u. is used as the frame for a spider web construction. The first mesh had elemental boundaries, on an axis through the center of the pyramid, of 0.04, 0.1, 0.2, and 0.4 a.u. For mesh 2 the boundaries are 0.08, 0.2, and 0.4 a.u., and for the third mesh 0.15 and 0.4 a.u. The pyramids were located in the inner cubic regions.

The results are presented to demonstrate the flexibility and robustness of the MSE method. Several benchmark calculations were presented in Ref. [4] for cubic and infinite domains to assess the resolution requirements and convergence of the MSE approach. Here focus is given to a molecular application as well as a systematic use of the domain decomposition method.

A. Hydrogenlike orbitals of nitrogen and zinc

The calculation of hydrogenlike orbitals of atomic nitrogen and zinc, $\hat{V}(x)=Z/r$, $Z=7$ and 30 in Eq. (5), are presented as a demonstration of the ability to systematically invert Schrödinger-type operators. The benchmark solution also offers the opportunity to systematically evaluate various mesh resolutions and requirements for obtaining chemical accuracy. The mesh consisted of a spider web structure within a cube of 0.8 a.u. in edge length, with the nuclei at its center. Three mesh refinements were examined, and are illustrated in Fig. 2; for mesh 1 the elemental boundaries, on an axis through the center of the pyramid, were 0.04, 0.1, 0.2, and 0.4 a.u. For mesh 2 the elemental boundaries were 0.08, 0.2, and 0.4 a.u., and for the third mesh they were 0.15 and 0.4 a.u. The pyramids were located in the inner cubic regions. All three domains had the same mid- and far-field skeleton meshes. The order of the polynomial approximation is varied to demonstrate exponential convergence for all meshes. Figure 3 illustrates the collocation mesh for the mesh 2 spider web on a two-dimensional plane through the center of the cubic region, as well as the entire domain skeleton mesh. The domain radius was 9 a.u., and this was taken as the practical infinity where the homogeneous Dirichlet boundary conditions were applied. The exact solution can readily be obtained analytically, and the eigenvalues are given by $\varepsilon_n=Z^2/2n^2$; the solutions $\propto e^{-Zr/n}$. The errors associated with the calculations of the first eigenvalues versus increasing polynomial order are plotted in Figs. 4 and 5, and exponential convergence rates were demonstrated; the $2s$ orbital gave slightly more accurate results, as reported in Ref. [4]. For the $Z=7$ results all meshes gave roughly equivalent results indicating the error was not dominated by the spider web region resolution, and higher resolution could be applied in the remaining domain. For the $Z=30$ solution meshes 1 and 2 gave equivalent results, while mesh 3 indicated that a finer elemental resolution is warranted, i.e., meshes 1 and 2, for the lower degree polynomial approximation to efficiently approximate the larger gradients in the s orbitals. Figure 6 plots the quadrature (collocation) points in the radial direction through the center of the elements for the three stated mesh refinements along with the normalized $1s$ orbitals. Multiresolution flexibility is demonstrated with higher resolution (smaller elements), near the nuclei, and the lower resolution (larger elements) in far-field region; 207 elements were used here.

Inversion of the global algebraic system was carried out by the preconditioned conjugate gradient method discussed above. Solutions were found to be fairly routine by the procedure discussed above, and 20 inner iterations were found to be an appropriate number. A few hundred global iterations were necessary to converge the orbitals to 10^{-10} errors in the residuals. Here the residual is defined as the L^2 norm of the

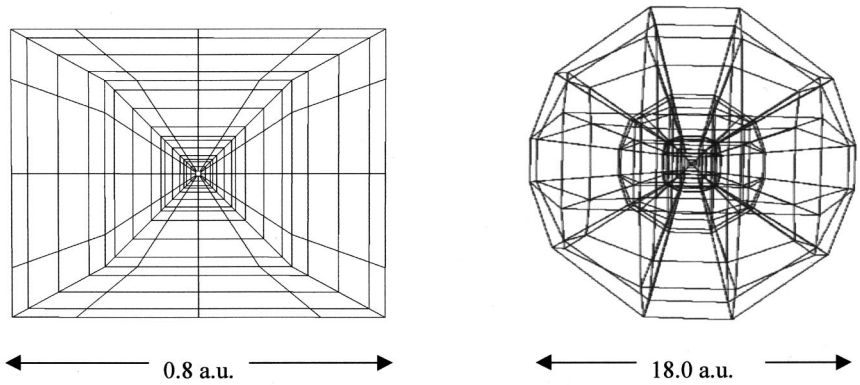

FIG. 3. Here a center plane is pictured with the collocation point grid laid out for a mesh-2-type spider web for $N=5$. To the right a complete spectral element spider web is presented. Typical domains will have rectangular regions decomposed in quadrilaterials, as pictured, and elliptical shells (or semi-infinite elements) placed around them.

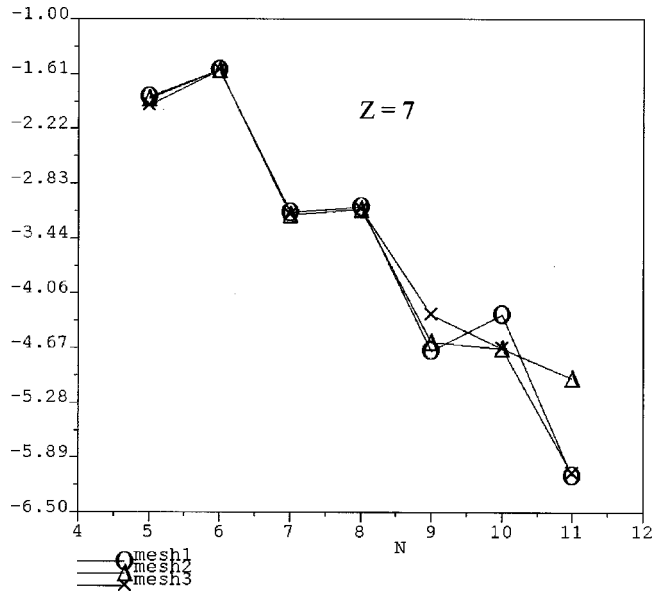

FIG. 4. The decay of the numerical error in the 1*s* orbital energy of the first hydrogenlike orbital of nitrogen is plotted vs the number of collocation points for the MSE solution; the three spider web mesh refinements considered are presented. The spherical-type domain was decomposed into 206 spectral elements, with six pyramids around the nuclei, and the domain radius for practical infinity was chosen as 9 a.u. Exponential convergence is demonstrated with a cusp present at the singularity location.

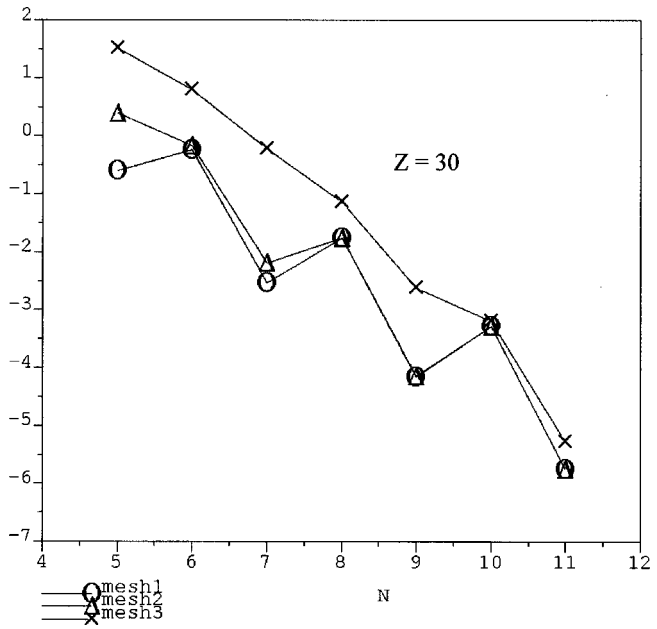

FIG. 5. The decay of the numerical error in the 1*s* orbital energy vs the number of quadrature points for the solution of the first hydrogenlike orbital of zinc are plotted here. The spherical-type domain was identical to that used for the nitrogen calculations reported above. Exponential convergence is demonstrated, with a cusp present at the singularity location, and resolution requirements are indicated for the increased gradients in the near nuclei region.

vector $(H-\varepsilon_i)\phi_i$, where H is Hamiltonian operator under study.

B. LDA results for atomic and diatomic systems

Here we present the results of $X\alpha$-VWN calculations for O, Ar, O_2, N_2, and F_2 at their experimental ground state configurations. For diatomic nitrogen the calculated exchange only $X\alpha$ ($\alpha=0.7$) orbital energies are presented along with a highly accurate calculation from a finite element solution using prolate-spheriodal coordinates [21]. The calculations of Ref. [21] imposed a practical infinity at 25 a.u., and utilized monopole potential boundary conditions. For the MSE approach a systematic mesh resolution around the nuclei was evaluated in a similar fashion as performed for the atomic calculations above. Here mesh 1 has near nuclei domain boundaries at 0.04, 0.1, 0.2, 0.5, and 1.0 a.u., mesh 2 at 0.08, 0.2, 0.5, and 1.0 a.u., and mesh 3 at 0.15, 0.4, and 1.0 a.u. The numerical error drops one order of magnitude from $N=7$ to 9, and represents an increase in total degrees of freedom by a factor 2.1. This convergence rate is consistent with those found in benchmark calculations reported in Sec. III A above, and in Ref. [4] for similar skeleton meshes. Here the exchange only LDA potential $V_x^{\mathrm{LDA}}(r)$ was used for comparison to the literature. Within each global iteration approximately ten inner iterations are performed for each orbital, and initial conditions were derived from one inverse iteration. All the orbitals were converged to residuals of 1×10^{-8}, and the electrostatic Coulomb potential was converged to 10^{-10} in its residual. There were a total of 282 spectral elements for the diatomic nitrogen calculation and the mesh had a radius of 20 a.u. With the mesh refinement used the addition of a nuclei requires adding 30 elements for mesh 1, 24 elements for mesh 2, and 18 elements for mesh 3 to the remaining unmodified skeleton mesh.

Several calculations were carried out to assess the sensitivity to multi-pole boundary conditions for the 20-a.u. domain. Calculations with mesh 1 and $N=7$ indicated that the monopole versus quadrupole boundary conditions change energies in the 10^{-4} hartree level; higher-order approximations resulted in lower total energy calculations. Table I presents the N_2 $X\alpha$ total and orbital energies for approximations $N=5$, 7, 9, and 11, for mesh 2, and those reported from Ref. [21]. The $N=11$ solution has the lowest total energy, and can be considered to be the most accurately computed LDA result for diatomic nitrogen; the results of Ref. [21] are limited

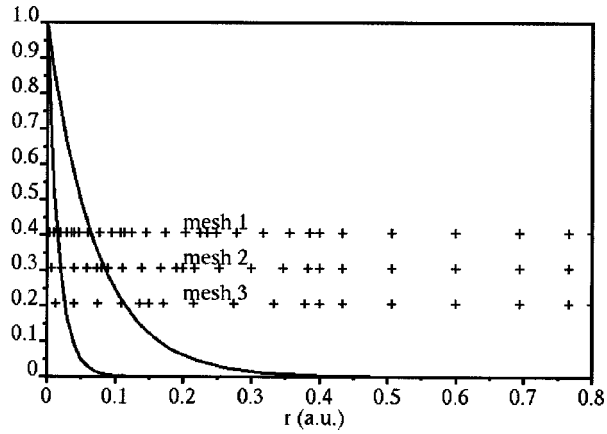

FIG. 6. A plot of the quadrature (collocation) points in the radial direction through the center of the elements for the three stated mesh refinements, along with the normalized 1*s* orbitals, for hydrogenlike solutions of nitrogen and zinc.

TABLE I. Computed Hartree-Fock-Slater orbitals of diatomic nitrogen by the MSE method for resolutions of five, seven, nine, and eleven collocation points in each spatial direction within the local spectral element. Comparison is given with accurate calculations using a prolate-spheriodal coordinate transformation, and a finite element method from Ref. [21].

MO	MSE, $N=5$ (hartree)	MSE, $N=7$	MSE, $N=9$	MSE, $N=11$	Ref. [21]	Orbital type
Total energy	−108.3339	−108.3440	−108.3464	−108.346 68	−108.34662	
1	−14.0089	−13.9823	−13.9811	−13.981 11	−13.981 11	$1\sigma_g$
2	−14.0076	−13.9809	−13.9797	13.979 70	−13.979 66	$1\sigma_u$
3	−1.0037	−1.0069	−1.0072	−1.007 22	−1.007 22	$2\sigma_g$
4	−0.4635	−0.4608	−0.4607	−0.460 73	−0.460 73	$2\sigma_u$
5	−0.4085	−0.4046	−0.4042	−0.404 24	−0.404 24	$1\Pi_u$
6	−0.4085	−0.4046	−0.4042	−0.404 24	−0.404 24	$1\Pi_u$
7	−0.3385	−0.3491	−0.3500	−0.350 06	−0.350 06	$3\sigma_g$

in solution accuracy due to the boundary conditions imposed. The accuracy of the various spider web skeleton meshes were in agreement with those for the atomic results above; changes in energies from mesh 1 to mesh 2 were in the 10^{-7} and 10^{-4}-hartree levels for mesh 1 to mesh 3. Additional LDA $X\alpha$-VWN ($\alpha=0.75$) calculations were also carried out for N_2 and gave a computed total energy of −110.639 hartree and a highest occupied molecular orbital (HOMO) of −0.540 hartree, without change in orbitals' symmetry type. The experimental ionization potential (IP) is 0.573 hartree, and the MSE-LDA results are in basic agreement with the predictive capability from single and doubly excited configuration interaction (CI) calculation, which gave an IP of 0.580 hartree, and second order perturbation results which gave an IP of 0.534 hartree [1].

Table II presents the post-LM gradient ($\alpha=\frac{2}{3}$) correction total energy, $X\alpha(\alpha=0.75)$-VWN total energy and HOMO energy, and the experimental ionization potential for the system studied here. Under appropriate asymptotic behavior of the functional DFT states, that the HOMO energy values should correspond to the measured IP, and the total energy will correspond to the same value as the full CI limit. All calculations were performed with an $N=9$ approximation, and a mesh-2-type refinement. In all the molecular calculations the LDA single particle equation correctly predicted the ground state symmetry, which includes the degenerate π_g^4 or HOMO for F_2; and in general all HOMO energies are within a few percent of the experimental IP. The qualitative drop in the IP for O_2 was also captured by the single particle LDA model. The dissociation energy of O_2 is overpredicted by approximately 7 eV, and is a common feature of LDA models; the closed shell LM post gradient correction reduced this overprediction to 2.7 eV. A more detailed comparison of various LDA models is given in Sec. III C, with the calculation of the ozone molecule.

TABLE II. Computed total energy with post-LMGC correction ($\alpha=\frac{2}{3}$) and the total energy and HOMO for the LDA-$X\alpha$VWN ($\alpha=0.75$) closed shell model for O, Ar, N_2, O_2, and F_2. The experimental ionization potential is given as well as the percent difference of the HOMO and experimental IP values. The calculations were all computed with a mesh-2 type near nuclei mesh and nine collocation point in each spatial direction per element ($N=9$).

	Total energy (hartree)	Total energy post-LMGC	HOMO (eV)	IP expt. (eV)	% error
O	−75.549	−75.834	14.142	13.6	4.0
Ar	−528.736	−529.570	14.597	15.8	7.6
N_2	−110.639	−110.982	14.697	15.6	5.8
O_2	−151.553	−151.958	10.060	9.5	5.9
F_2	−227.384	−201.446	14.467	15.6	7.3

C. Local density functional results for ozone

Ozone has many interesting characteristics with regards to its theoretical and computational study. There is an extensive amount of literature on the theoretical predictions of ozone; early LCAO efforts (1968–1979) were discouraging, and found 60° geometries with lowest energy. LCAO basis-set incompleteness has been a dominant issue in ozone's history of theoretical study. In fact, there has been nearly 30 years of research discussing the need to included *d* polarization functions in basis sets for a molecule as small as ozone, and these basis sets still offer suspect results in various physical observables and absolute energies. The MSE method eliminates this issue entirely, and allows the examination of various DFT models without the concern of basis-set incompleteness and its associated errors.

Single determinant Hartree-Fock calculations have proven to be insufficient due to the noted radical character of the ground state. The diffused character of the electron distribution combined with a rapidly varying wave function in the near nuclei region, and the highly degenerate energy states of the molecular orbitals, have also proven to be a formidable challenge for numerical approximation. A timely review of the theoretical study of ozone can be found in Hay and Dunning [56]; there generalized valence bound (GVB) orbital structures are presented, along with detailed studies of the excited states for minimal chemical basis-set calculations. The authors of Ref. [57], with a $(9s/5p/1d)$ basis set and the VWN LDA model, indicated that the open form gave good geometry comparisons to experiment; $X\alpha$-SW calculations are in similar agreement. Jursic [58] performed an extensive study on various DFT models on ozone, and found

TABLE III. Here several calculations of the LDA-$X\alpha$ ($\alpha=0.74$) are presented for cyclic and experimental ground state geometries of ozone at different spectral element resolutions. The calculations are presented to demonstrate numerical and chemical accuracy of the calculation. At $N=7$ chemical accuracy is achieved in the sense that the correct energetic order of the geometries is captured. A further increase in N shows the characteristics associated with the variational formulation, i.e., convergence is from above. The table presents total energies, the lowest energy ($1s$) orbital, and the HOMO and its nearest occupied orbital.

MSE $X\alpha$ ($\alpha=0.74$)	$N=5$ (hartree)	$N=7$	$N=9$
116.8°, $R=1.278$ Å			
Total energy, E_T	−224.137	−224.674	−224.737
ε_1	−19.172	−19.057	−19.048
ε_{11}	−0.285	−0.292	−0.293
ε_{12} (HOMO)	−0.281	−0.288	−0.290
60°, $R=1.44$ Å			
Total energy	−224.485	−224.635	−224.675
ε_1	−18.976	−18.925	−18.921
ε_{11}	−0.273	−0.261	−0.262
ε_{12} (HOMO)	−0.267	−0.261	−0.262
$E_{T,116}-E_{T,60}$	0.34	−0.04	−0.06

that geometry optimization was rather straightforward with the GAUSSIAN92 implementation of density functional methods. Jursic's results indicated that the non-local Becke-Lee-Yang-Parr combinations of exchange and correlation corrections, and a 6-$31G(d,p)$ basis set, gave the best comparison to experiment.

Here an extensive numerical study of ozone was carried out with the (60°, $R=1.44$ Å) cyclic configuration and the (116.8°, $R=1.278$ Å) experimental ground state configuration for the LDA-KS exchange only $X\alpha$ potential ($\alpha=0.74$), the empirical GL correlation correction in the Dirac exchange limit ($\alpha=\frac{2}{3}$), and the VWN model with Dirac-Slater ($\alpha=1.0$) exchanges, and empirical exchange ($\alpha=0.74$ and 0.75). The suggested optimal α for atomic oxygen is 0.744. Several domains and polynomial orders were used here to measure the sensitivity of the solution on grid resolution; in general all meshes used gave equivalent results to stated accuracy. The final mesh consisted of a total of 234 spectral elements for the ground state geometry with an effective domain radius of 20 a.u. and a near nuclei spider web construction similar to a mesh 2 type (see above), with element edges at 0.08, 0.24, and 0.54 a.u. A resolution study for the two geometries is presented in Table III, where total energies and selected orbital energies are reported for $N=5$, 7, and 9 collocation points in each spatial direction in each element; in general the addition of 2 in polynomial order represents an order of magnitude decrease in numerical error. A representative spectral element mesh consisting of 306 elements is presented in Fig. 7, with color contours of the electronic density for a cyclic geometry. Extensive calculations were carried out to test the computational accuracy; domains of 17–27 a.u. in radius were studied for application of practical infinity; changes in the fourth decimal point were found in orbital energies for these cases. Multipole expansions used for the application of Coulomb potential far-field boundary conditions, from dipole to quadrupole moments, gave 10^{-4} hartree effects; all results stated are with quadrupole boundary conditions. All calculations and all LDA models, at all resolutions, gave the same qualitative orbital structures, and the correct energetic order of the two geometries was reached at $N=7$. The $N=7$ versus $N=9$ results changed at the 10^{-2} hartree level for the total energy and lowest orbital energies, and at the 10^{-3} hartree level in the HOMO and its nearest orbitals' energies; $N=9$ can therefore be expected to be approximately one order of magnitude lower than this error, and chemical accuracy is thus stated. The results of the orbital energies are given in Table IV for the $X\alpha$-VWN ($\alpha=0.74$) approximations for the cyclic form $N=9$, and the ground state geometry for $N=7$ and 9.

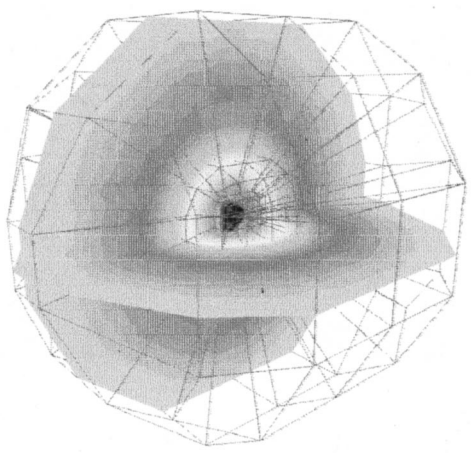

FIG. 7. The LDA-MSE computational mesh of ozone (60°, 1.44 a.u.), and the computed Coulomb potential, are plotted within the MSE skeleton mesh. The skeleton mesh structure is typical of all grids used for calculations reported in this paper.

The results of all LDA models for the $N=9$ calculations indicated that the ground state geometry is approximately 0.06 hartree lower than the cyclic form. Table V presents a comparison of the total energies and calculated HOMO energies for the MSE-LDA models as well as the experimental ionization potentials. Figure 8 plots the color contours of the MSE-LDA molecular orbitals 10, 11, and 12 in the region local to the nuclei for the (116.8°, $R=1.278$ Å) ground state geometry. Finally, Fig. 9 presents illustrative orbital structures for all MSE LDA orbitals and the six highest calculated orbitals from the LCAO-VWN ($9s/5p/1d$), and $X\alpha$-SW methods; for all high-precisiion MSE-LDA calculations the qualitative structure of the orbitals was invariant with the DFT model and computational resolution. The LCAO-VWN ($9s/5p/1d$) calculations have approximately a numerical error in the total energy of 3.3 hartree (90 eV) as compared to the accurate MSE results.

The lowest total energy found in the literature was from a large multiconfiguration self-consistent-field (MCSCF) calculation [59], and was −224.65 hartree. The $X\alpha$ ($\alpha=0.74$) exchange approximation, combined with the VWN correlation model, gave a total energy of −227.387 hartree and less then a 2% difference between the experimental ionization potential of 0.469 a.u. (12.75 eV) and the calculated HOMO. The accuracy of the MSE-LDA prediction of the IP

TABLE IV. Computed total and orbital energies for the LDA $X\alpha$-VWN model for ozone are presented; here the Dirac theoeretical limit $\alpha=\frac{2}{3}$ is reported for accurate MSE results. The MSE calculations reported are for nine quadrature points in each spatial direction for each spectral element; $N=9$ for the cyclic form, and $N=7$ and 9 for the ground state structutre. Comparisons are appropriate for equal values of N since this factor represents roughly equivalent numerical errors for general skeleton mesh constructions.

Orbital	Orbital energy (60°, $R=1.44$ Å) MSE-VWN ($N=9,\alpha=\frac{2}{3}$)	(hartree) (116.8°, $R=1.278$ Å) MSE-VWN ($N=7,\alpha=\frac{2}{3}$)	(116.8°, $R=12.78$ Å) MSE-VWN ($N=9,\alpha=\frac{2}{3}$)
Total energy	−227.336	−227.333	−227.396
1	−18.921	−19.058	−19.048
2	−18.921	−18.885	−18.872
3	−18.921	−18.885	−18.872
4	−1.343	−1.380	−1.379
5	−0.951	−1.129	−1.128
6	−0.951	−0.832	−0.830
7	−0.640	−0.673	−0.673
8	−0.597	−0.667	−0.666
9	−0.585	−0.655	−0.656
10	−0.585	−0.461	−0.642
11	−0.389	−0.418	−0.420
12	−0.389	−0.414	−0.416

is at the same level as the MCSCF-CI results stated in Ref. [60]. Several researchers have indicated that the largest error in the LDA approximation is with the exchange energy [19]. The various $X\alpha$ exchange adjustments with Dirac-Slater and empirical α constants indicate that the high precision MSE-$X\alpha$-VWN LDA results agree with the correct experimental ground state structure as well as the experimental IP, with an optimal α consistent with that suggested from literature. However, the ground state dissociation energy is overestimated by approximately the same amount as the O_2 dissociation energy. Generalized gradient corrections to the Dirac exchange limit are expected to offer an accurate multipurpose model and are under consideration.

TABLE V. Here various total energies and HOMO values are report for the MSE-LDA-$X\alpha$, VWN, and GL models. Comparisons are made to those reported in the literature, and percent errors are given with respect to the experimentally measured ionization potential (IP); for the MSE results the IP is taken to be approximated by the HOMO. Use of the suggested optimal α for atomic oxygen (0.744) gives an error in the IP of less then 2% for the closed shell MSE-LDA calculation, and this is of the same level of error as a large LCAO-MCSCF calculation reported in Ref. [60].

Computational method	Total energy (hartree)	IP (HOMO) (eV)	% error in IP
MSE $X\alpha$ ($\alpha=.74$) 116.8°, $R=1.278$ Å	−224.737	7.891	38.2
MSE $X\alpha$-GL ($\alpha=\frac{2}{3}$)	−227.420	8.490	33.5
MSE $X\alpha$-VWN ($\alpha=\frac{2}{3}$)	227.396	11.320	11.3
MSE $X\alpha$-VWN ($\alpha=\frac{2}{3}$) post-LMGC correction	−228.243		
MSE $X\alpha$-VWN ($\alpha=0.74$)	−227.387	12.463	2.3
MSE $X\alpha$-VWN ($\alpha=0.75$)	−227.384	12.599	1.2
MSE $X\alpha$-VWN ($\alpha=1.0$) Open form, Ref. [57]	−227.205	16.925	32.6
LCAO/VWN,9s/5p/1d 117.5°, $R=1.27$ Å	−223.946	6.1	52.2
$X\alpha$-SW, Ref. [57]		8.1	36.5
$X\alpha$-SW, Ref. [60]		12.79	0.2
GVB-CI, Ref. [60]		12.91	1.2
MCSCF+CI, Ref. [50]		12.53	1.8

Several advantages are indicated from the accurate closed shell MSE computation. The degenerate HOMO for the 60° structure is retained to the third decimal point for the 116.8° case; this is nearly captured by the $X\alpha$-SW simulation, but not by the LCAO. The general agreement in IP prediction was previously found only in higher level correlation treatments; here highly accurate calculations indicate that the LDA is adequate to a few percent accuracy. Accurate MSE results indicate that the (116.8°, $R=1.278$ Å) structure is lower in energy then the (60°, $R=1.44$ Å) structure by an amount of 0.06 hartree (1.6 eV) for all LDA models examined; this is comparable to the open shell predictions of LCAO-VWN calculations with a 0.07-hartree difference. The difference in total energies of the ground state and cyclic geometries was found to be insensitive to the skeleton mesh construction and LDA model, for a given number of collocation points (N). The high-precision MSE calculations offer a numerically accurate prediction of the modeled band structure of the orbital energies for the highest orbitals; considerable disagreement exists with the various LCAO methods. In fact, Fig. 9 indicates a qualitative disagreement of the LCAO highest six orbital wave functions and their symmetries when compared to the highly accurate Kohn-Sham MSE-LDA orbitals; the experimental ground state is $^1A_1$. The LDA-MSE orbitals indicate that there are two occupied π orbitals perpendicular to the molecular plane. LCAO-LDA calculations do not predict this type of symmetry; GVB orbitals have

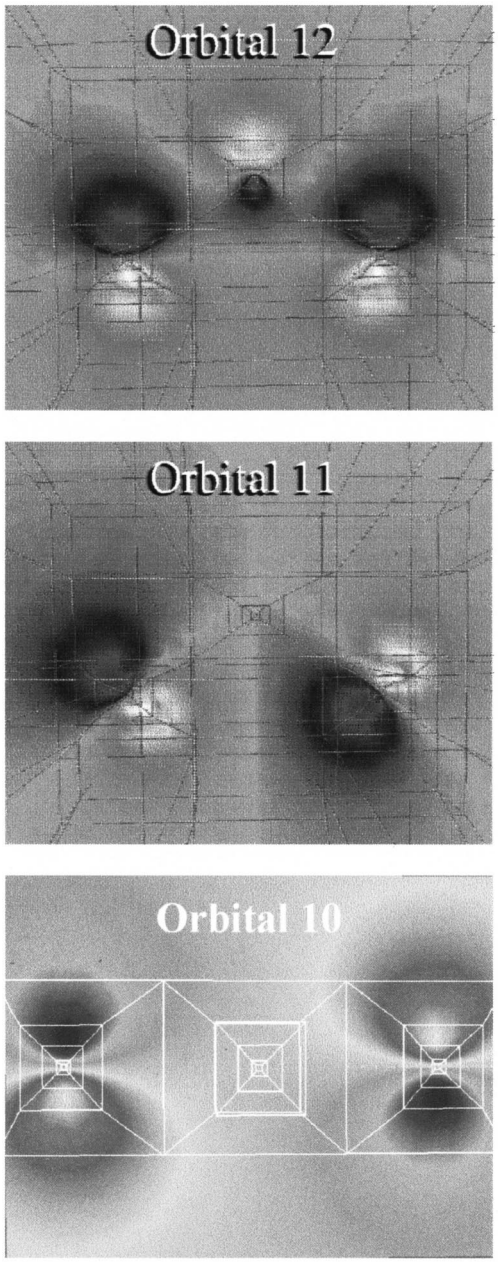

FIG. 8. MSE-LDA molecular orbitals 10, 11, and 12 of ozone ($116.8°, R=1.278$ Å) are plotted above. One of the two occupied π orbitals perpendicular to the molecular plane is pictured in orbital 10 (bottom). The computational solution was taken from a GL calculation, with a spider web construction representative of a mesh-1-type decomposition; see Sec. III A.

planar π orbitals, though with different structural symmetry [55]. Detailed electronic structure properties such as excited states, ionization potentials, adiabatic excitation energies, etc., can all be considered to be strongly dependent on the accuracy of the computation and the DFT model in this part of the spectrum; the numerical accuracy capability is effectively provided with modern spectral methods. Although qualitative study of molecular orbitals has lost favor over the last decade, the ability to calculate robust and reliable wave functions is expected to offer new directions for wave function analysis [3].

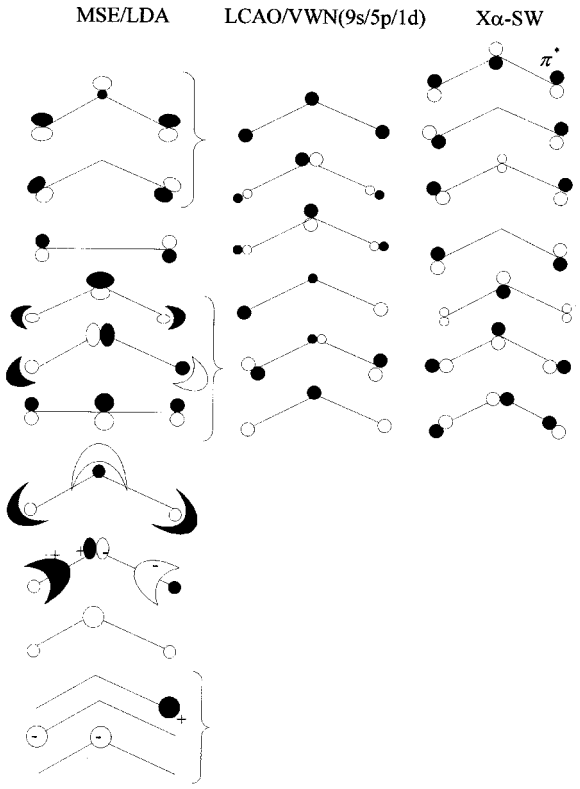

FIG. 9. Highly accurate Kohn-Sham MSE-LDA (left) molecular orbitals for ozone ($116.8°, R=1.278$ Å) are compared to the LCAO-LDA results with a ($9s/5p/1d$) basis-set (middle) [57], and the $X\alpha$-SW results (right) [60]; the brackets indicate nearly degenerate orbital energies. In the LCAO-$X\alpha$ results the $\xi^*(b1)$ orbital is unoccupied in the ground state.

IV. SUMMARY

The increasing need for advanced computational modeling capabilities for material design and property prediction, in both material science and molecular chemistry, requires the development of new theoretical and computational methods. Here we presented a computational approach for use in high-precision multicenter electronic structure calculations, and demonstrate that *p*-type finite elements are a viable numerical approach to many electron systems with highly nonlinear functionals and strongly nonspherically symmetric wave functions in the near nuclei region. In particular, the local interpolant formulation and a higher-order quadrature allows the physical space formulation to routinely evaluate advanced gradient corrections, both variational and pointwise constraints [61], to the LDA in a fully self-consistent manner. The method can be viewed as an extension of the spectral element method developed to solve elliptical partial differential equations. Evaluations of the Hamiltonian operation scale to be linear in the number of elements, which is proportional to number nuclei, and proportional to N^4, where N is the local polynomial expansion order in one spatial direction for a given element. Successful numerical approximations of operators with point singularities was accomplished with the use of a local coordinate transformation, and allow general multicenter systems to be calculated with a higher-order finite element method that give spectrally accurate numerical solutions. Optimal iterative solvers can be expected to offer linear scalability in the number of electrons as

well. Thus the potential for a total linear scalable numerical algorithm for a high-level quantum chemical calculation is realistically possible within the state of the art in modern iterative solutions. The numerical approximation consistently deals with a full theoretical statement, and accurately captures the correct balance of the kinetic energy and divergent terms.

The computational method offers the unambiguous assessment of various theoretical approximatiions to multicenter systems in a computationally tractable fashion. Advantages can be found for problems currently intractable due to multicenter complexity; large basis set expansions, rapidly varying wave functions, and computationally intensive many electron applications. The combination of multiresolution flexibility and exponential convergence rates yields a computationally efficient technique for solving Schrödinger-type operators, and advances in algorithms and iterative solvers for partial differential equations will transfer seamlessly between the various multidisciplinary areas of computational physics.

Here computations of a subset of atomic, diatomic, and triatomic systems were studied to validate and apply the method to electronic structure calculations. The studies indicated a general ability of the VWN model to give a HOMO energy to within a few percent of the experimental ionization energy. The highly accurate and robust calculations of the MSE method proved to offer a significantly different picture of LDA molecular orbitals than that provided by LCAO methods for ozone. The accuracy of the MSE-LDA prediction of the IP is at the same level as MCSCF-CI results reported in the literature, and gave less than a 2% difference between the experimental ionization potential. In general all LDA models, at all resolutions, gave the same qualitative orbital structures. For ozone the correct energetic order of the ground state versus the cyclic geometries was also predicted with all closed shell LDA models studied here. Applications are currently being studied for large-scale molecular structures and optimal iterative solvers for several hundred atoms and electrons in the context of density functional theory. In addition to the molecular orbital studies presented here, highly accurate numerical solutions can be expected in connection with the work on the density equation [62–65]. Likewise, the ability to deal with approximations of wave functions for heavy nuclei, in an all electron calculation, and incorporation of relativistic effects, such as Dirac's equation [66,2], are apparent. Although Dirac's equation was not formally addressed in this paper, the MSE approach is expected to have a meaningful application direction here. LCAO methods are known to have limited merits over fully numerical solutions of Dirac's equation at the atomic level [67]. The application of modern spectral methods is expected to benefit calculations in nuclear physics as well as scattering.

ACKNOWLEDGMENTS

The author would like to thank Professor Leland C. Allen and Dr. Brett I. Dunlap for several informative discussions. Also appreciation is noted for the encouragement the author received from Professor Ioannis G. Kevrekidis at the early stages of the work

[1] A. Szabo and N. S. Ostlund, *Modern Quantum Chemistry; Introduction to Advanced Electronic Structure Theory* (McGraw-Hill, New York, 1989).
[2] W. Jones and N. M. March, *Theoretical Solid State Physics* (Wiley, New York, 1973), Vol. 1.
[3] M. Head-Gordon, J. Phys. Chem. **100**, 13 213 (1996).
[4] P. F. Batcho, Phys. Rev. A **57**, 4246 (1998).
[5] J. D. Morgan, in *Numerical Determination of the Electronic Structure of Atoms, Diatomics, and Polyatomic Molecules*, edited by M. Defranceschi and J. Delhalle (Kluwer, Dordrecht, 1988).
[6] J. Kobus, Chem. Phys. Lett. **202**, 7 (1993).
[7] L. Laaksonen, P. Pyykko, and D. Sundholm, Comput. Phys. Rep. **4**, 313 (1986).
[8] P. Pyykko, in *Numerical Determination of the Electronic Structure of Atoms, Diatomics, and Polyatomic Molecules* (Ref. [5]).
[9] D. Moncrieff and S. Wilson, J. Phys. B **27**, (1994).
[10] D. Gottlieb and C. W. Shu, SIAM Rev. **39**, 4 (1997); **39**, 644 (1997).
[11] D. Gottlieb and S. A. Orszag, *Numerical Analysis of Spectral Methods: Theory and Applications* (SIAM, Philadelphia, 1977).
[12] A. T. Patera, J. Comput. Phys. **54**, 468 (1984).
[13] Y. Maday and A. T. Patera, in *State of the Art Surveys in Computational Mechanics*, edited by A. Noor (American Society of Mechanical Engineers, New York, 1987).
[14] E. M. Ronquist, Ph. D. Thesis, Massachusetts Institute of Technology, 1988 (unpublished).
[15] P. Honenberg and W. Kohn, Phys. Rev. B **136**, 864 (1964).
[16] W. Kohn and L. J. Sham, Phys. Rev. A **140**, 1133 (1965).
[17] *Density Functional Theory of Molecules, Clusters, and Solids*, edited by D. E. Ellis (Academic, New York, 1995).
[18] *Chemical Applications of Density Functional Theory*, edited by B. B. Laird, R. B. Ross, and T. Ziegler, ACS Symposium, 1996 (American Chemical Society, Washington D.C., 1996), Series 629.
[19] R. G. Parr and W. Yang, *Density Functional Theory of Atoms and Molecules* (Oxford University Press, Oxford, 1989); W. Kohn, A. D. Becke, and R. G. Parr, J. Phys. Chem. **100**, 12 974 (1996).
[20] B. I. Dunlap, Int. J. Quantum Chem. **64**, 193 (1997).
[21] D. Heinemann, B. Fricke, and D. Kolb, Phys. Rev. A **38**, 4994 (1988).
[22] S. R. White, J. W. Wilkins, and M. P. Teter, Phys. Rev. B **39**, 5819 (1989).
[23] F. S. Levin and J. Shertzer, Phys. Rev. A **32**, 3285 (1985).
[24] E. Tsuchida and M. Tsukada, Solid State Commun. **94**, 5 (1995).
[25] J. Ackermann, B. Erdmann, and R. Roitzsch, J. Chem. Phys. **101**, 7643 (1994).
[26] H. Murakami, V. Sonnad, and E. Clementi, Int. J. Quantum Chem. **42**, 785 (1992).
[27] H. Yu and A. D. Bandrauk, J. Chem. Phys. **102**, 1257 (1995).

[28] S. Goedecker, Rev. Mod. Phys. **71**, 1085 (1999).
[29] P. E. Maslen, C. Ochsenfeld, C. A. White, M. S. Lee, and M. Head-Gordon, J. Phys. Chem. A **102**, 2215 (1998).
[30] E. Hernandez and M. J. Gillan, Phys. Rev. B **53**, 7147 (1996).
[31] X. P. Li, R. W. Nunes, and D. Vanderbilt, Phys. Rev. B **47**, 16 (1993); **47**, 10 891 (1993).
[32] T. A. Arias, Rev. Mod. Phys. **71**, 269 (1999).
[33] N. A. Modine, G. Zumbach, and E. Kaxiras, Phys. Rev. B **55**, 10 289 (1997).
[34] R. A. Friesner, Annu. Rev. Phys. Chem. **42**, 1341 (1991).
[35] A. D. Becke and R. M. Dickson, J. Chem. Phys. **92**, 3610 (1991); A. D. Becke, *ibid.* **107**, 8554 (1997).
[36] P. F. Batcho, G. E. Karniadakis, and S. A. Orszag, J. Fluids Struct. **5**, 681 (1991).
[37] P. F. Batcho and G. E. Karniadikis, Phys. Fluids A **3**, 1051 (1991).
[38] P. F. Batcho, Ph.D. Thesis, Princeton University, 1994 (unpublished).
[39] P. F. Batcho and G. E. Karniadakis, J. Comput. Phys. **115**, 121 (1994).
[40] A. Ghizzetti and A. Ossicini, *Quadrature Formulae* (Academic, New York, 1970).
[41] S. Sherwin, Ph.D. thesis, Princeton University, 1995 (unpublished); S. J. Sherwin and G. E. Karniadakis, J. Comput. Phys. **124**, 14 (1996).
[42] Y. Maday and R. Munoz, J. Sci. Comput. **3**, 323 (1988).
[43] I. Stich, R. Car, M. Parinello, and S. Baroni, Phys. Rev. B **8**, 4997 (1989).
[44] M. C. Payne, M. P. Teter, D. C. Allan, T. A. Arias, and J. D. Joannopoulos, Rev. Mod. Phys. **64**, 4 (1992).
[45] M. P. Teter, M. C. Payne, and D. C. Allan, Phys. Rev. B **40**, 18 (1989).
[46] S. Costiner and S. Ta'asan, ICASE Report 94-91 (ICASE, Virginia, 1994); Phys. Rev. E **51**, 3704 (1995); **52**, 1181 (1995).
[47] E. L. Briggs, D. J. Sullivan, and J. Bernholc, Phys. Rev. B **52**, 5471 (1995); F. F. Grinstein, H. Rabitz, and A. Askar, J. Comput. Phys. **51**, 423 (1983).
[48] K. Davstad, J. Comput. Phys. **99**, 33 (1992).
[49] *Linear and Nonlinear Conjugate Gradient Related Methods*, edited by L. Adams and J. L. Nazareth (SIAM, Philadelphia, 1996).
[50] R. B. Lehoucq, D. C. Sorensen, and C. Vang, *Solution of Large Scale Eigenvalue Problems with Implicitly Restarted Arnoldi Methods* (SIAM, Philadelphia, 1998).
[51] L. F. Pavariono and O. B. Widlund, Int. J. Comput. Math. Appl. **33**, 193 (1997).
[52] P. M. Morse and H. Feshbach, *Methods of Mathematical Physics I* (McGraw Hill, New York, 1953).
[53] L. Greengard and V. Roklin, Acta Numerica **6**, 2298 (1997).
[54] O. Gunnarsoon and B. I. Lundqvist, Phys. Rev. B **13**, 4274 (1976).
[55] S. H. Vosko, L. Wilk, and M. Nusair, Can. J. Phys. **58**, 1200 (1980); G. S. Painter, Phys. Rev. B **24**, 4264 (1981).
[56] P. J. Hay and T. H. Dunning, Jr., J. Chem. Phys. **67**, 2290 (1977).
[57] M. Morin, A. E. Foti, and D. R. Salahub, Can J. Chem. **63**, 1982 (1985).
[58] B. S. Jursic, J. Mol. Struct.: THEOCHEM **389**, 251 (1997).
[59] W. D. Laidig and H. F. Schaefer, J. Chem. Phys. **74**, 3411 (1981).
[60] R. P. Messmer and D. R. Salahub, J. Chem. Phys. **65**, 779 (1976).
[61] R. Newmann, R. H. Nobes, and N. C. Handy, Mol. Phys. **97**, 1 (1996).
[62] G. Hunter, Int. J. Quantum Chem. **XXIX**, 197 (1986).
[63] D. A. Mazziotti, Phys. Rev. A **57**, 4219 (1998).
[64] M. Levy and H. O. Yang, Phys. Rev. A **38**, 2 (1988).
[65] N. H. March, Int. J. Quant. Chem., Quantum Bio. Symp. **13**, 003 (1986).
[66] L. I. Schiff, *Quantum Mechanics*, 3rd ed (McGraw-Hill, New York, 1968).
[67] P. Pyykko, Chem. Rev. **88**, 563 (1988).